Chapter 3

Phase Identification and Size Evaluation of Mechanically Alloyed Cu-Mg-Ni Powders

Celal Kursun, Musa Gogebakan,
M. Samadi Khoshkhoo and Jürgen Eckert

Additional information is available at the end of the chapter

http://dx.doi.org/10.5772/67404

Abstract

Ternary mixture of Cu, Mg, and Ni with the nominal composition of nanocrystalline $Cu_{50}Mg_{25}Ni_{25}$ (in at.%) was milled for 25 hours. Analysis of an X-ray diffraction pattern (XRD) and transmission electron microscopy (TEM) was used to characterize the chemical phases and microstructure of the final product, which is shown to consist of ternary alloy of Cu-Mg-Ni with FCC structure along with small amounts of FCC MgO and $Mg_{0.85}Cu_{0.15}$. The good agreement between the size values obtained by XRD and TEM is attributed to the formation of defect-free grains with no substructure during ball milling. Dynamic recrystallization may be a possible mechanism for the emergence of such small grains (<20 nm). The particle size distribution and morphological changes of Cu–Mg–Ni powders were also analyzed by scanning electron microscopy (SEM). According to the SEM results, the particle size of the powders decreased with increasing milling time. Lattice parameter of the Cu-Mg-Ni ternary FCC alloy formed during mechanical alloying increased with increase in milling time from 3.61 to 3.65 Å after 20 hours milling.

Keywords: nanocrystalline powders, Cu-Mg-Ni alloy, mechanical alloying, Rietveld, TEM

1. Introduction

High strength and good electrical and thermal conductivities are the fundamental requirements for materials in electrical industries [1]. Copper-based alloys are the optimal materials for such applications [2]. There are certain methods to fabricate these materials such as mechanical alloying, vapor deposition, rapid solidification, etc. In mechanical alloying, materials are obtained in powder form, which can be later compacted to desired shapes and

dimensions for practical applications. The advantage of mechanical alloying is the possibility and easy production of super saturated solid solutions and meta-stable phases that is generally difficult to obtain from other techniques [3, 4]. Thus, many studies have been devoted to the production of meta-stable materials that are amorphous, nanocrystalline, and quasicrystalline by using mechanical alloying.

Mechanical and physical properties of materials strongly depend on their grains size [5, 6]. A lot of studies have been carried out to enlighten the relationship between the microstructure and mechanical and physical properties [7–10]. For this purpose, determination of grain size is of great importance. Transmission electron microscopy (TEM) investigation, that is based on direct observations and counting of the grains [11], provides grain size and grain size distribution, which is closer to the reality. However, due to the ease of X-ray diffraction technique, this method has been used extensively to determine the size of the coherent domains in nanomaterials. Size evaluation using X-ray diffraction pattern (XRD) is based on the broadening of reflections in diffraction pattern. Usually, there is a large discrepancy between the results obtained by TEM and XRD [12]. This discrepancy originates from the difference between the type of the information obtained by XRD and TEM. In fact, the size value obtained by TEM and XRD corresponds to grain size and coherently scattering of domain size. Depending on the processing route, both these values can be near or far from each other. There are several methods to obtain coherent domain size and microstrain from the X-ray diffraction patterns including Williamson-Hall, Halder-Wagner, Warren-Averbach, Debye-Scherrer, and Rietveld refinement method [13]. In the present work, the microstructure of the final powder is investigated using transmission electron microscopy (TEM), Debye-Scherrer equation, and Rietveld refinement of X-ray diffraction (XRD) patterns. The good agreement obtained between the results of XRD and TEM will be discussed in terms of the possible microstructural evolutions during mechanical alloying.

2. Experimental

Ternary Cu-Mg-Ni powder alloy with the nominal composition of $Cu_{50}Mg_{25}Ni_{25}$ was mechanically alloyed in planetary ball mills (Fritsch Pulverisette 5). The elemental powders of Cu, Mg, and Ni were accurately weighted to the desired compositions. Powders together with stainless steel milling balls were charged into a stainless steel vial (125 mL). Ball milling was performed at room temperature at the rotation speed of 300 rpm with a ball to powder mass ratio (BPR) of 10:1. The powders were mechanical alloyed up to 25 hours. After each 15 minutes of ball milling, the process was interrupted for 30 minutes in order to cool down the vials. Samples were taken at suitable milling times to follow the changes of microstructure and phases during ball milling.

Phase transformation during milling was studied using X-ray diffraction (XRD) analysis. For this purpose, a diffractometer with Co Kα radiation operating at 40 kV was employed. The crystallite size determination was performed using diffraction pattern obtained by a STOE Stadi P diffractometer (CuKα1 radiation) operating at 40 kV in transmission geometry with small instrumental broadening. The diffraction patterns were recorded using a linear position sensitive detector with the 2θ (diffraction angle) range of 30–130^{o}. TEM investigations of the final product were performed using a Phillips CM-20 transmission electron microscope operating at 200 kV.

http://dx.doi.org/10.5772/67404

3. Results and discussion

Figure 1 shows the X-ray diffraction patterns of $Cu_{50}Mg_{25}Ni_{25}$ powder at different milling times using X-ray source wavelength = 0.154056 nm. The reflections corresponding to the starting materials Cu, Mg, and Ni are broadened and fade away only after 5 hours of milling as shown in **Figure 1(a)**. The elemental Cu peaks decrease more rapidly than Ni peaks, indicating faster grain size refinement in the Cu powders. Similar observation is reported by Gogebakan et al. for the $Al_{65}Cu_{20}Fe_{15}$ [14]. The main reflections of Ni and Cu become closer to each other and form a single broad reflection in the 2θ range of 45–55°. This happens due to the fact that mechanical alloying pumps the atoms of the existing elements into the lattice of each other, leading to the opposite shift in the peak positions of Ni and Cu. As a result, initial crystals are also heavily strained that leads to the broadening of the reflections. On the other hand, grain refinement occurs during ball milling that causes the additional broadening of the reflections. A rough modeling of the XRD pattern using Rietveld analysis for 5 hours of milling showed that the observed broad peak for $Cu_{50}Mg_{25}Ni_{25}$ can be attributed to the (111) reflection of an FCC structure (in this case Cu-based solid solution) with coherently scattering domain.

On further milling, the broad reflection became sharper and the other reflections of lower intensity appeared. As shown in **Figure 1(b)**, finally after 25 hours of milling, the structure is composed of a Cu-based FCC structure along with a minor amount of MgO and $Mg_{0.85}Cu_{0.15}$ intermetallic. They are marked by symbols in **Figure 1(b)**.

X-ray diffraction pattern of the final powder (milled for 25 hours) was modeled using Rietveld refinement. A good agreement was obtained between the experimental and calculated patterns as shown in **Figure 2**. Only the effects of size and strain were considered during the refinement with no special corrections for the effect of planar lattice defects as well as strain anisotropy. The size values obtained for the Cu-based FCC solid solution, $Mg_{0.85}Cu_{0.15}$ intermetallic, and MgO are 10, 10, and 15 nm, respectively.

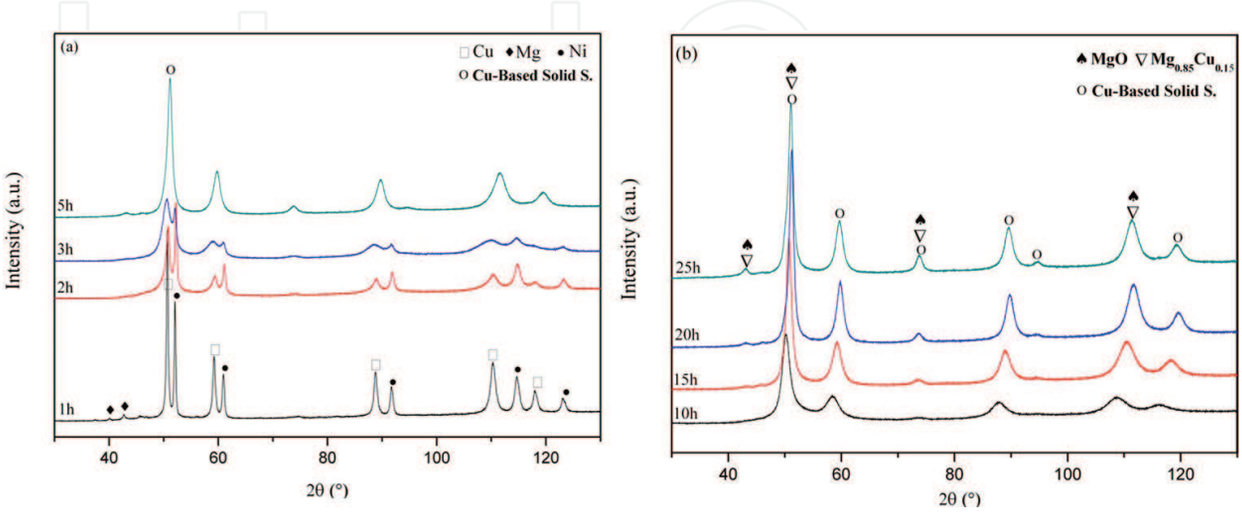

Figure 1. XRD patterns of $Cu_{50}Mg_{25}Ni_{25}$ alloy after different milling time; (a) 1–5 hours, (b) 10–25 hours.

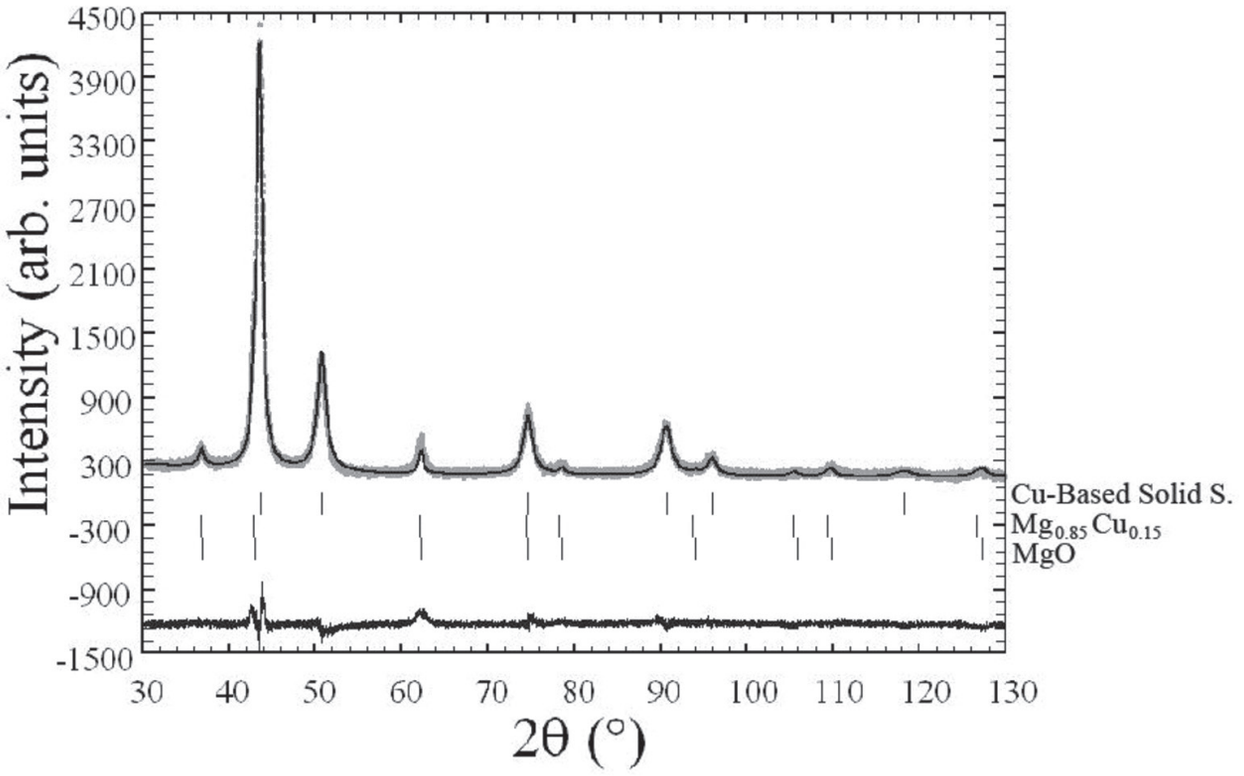

Figure 2. Rietveld refinement for XRD patterns of $Cu_{50}Mg_{25}Ni_{25}$ powders after 25 hours of milling time.

The crystallite size evolution of the $Cu_{50}Mg_{25}Ni_{25}$ powder alloy as a function of milling time is presented in **Figure 3**. The variation of crystallite size of the powder alloy was estimated by broadening of XRD peaks using Debye-Scherrer equation [15]

$$D = \frac{0.9\lambda}{B\cos\theta} \tag{1}$$

where D is the average crystallite size, λ is the wave length of using X-ray, B is the full width (in radians) at half maximum intensity, and θ is the diffraction Bragg angle.

As seen in **Figure 3**, the crystallite size of the ternary FCC Cu-Mg-Ni alloy is found to decrease initially with increase in milling time approaching near saturation after 10 hours of milling. It was calculated to be about 30, 18.5, 19, and 17 nm after 5, 10, 15, and 20 hours milling, respectively, and reached a steady-state value of about 17 nm after 25 hours of milling.

The morphological changes of the $Cu_{50}Mg_{25}Ni_{25}$ alloy during mechanical alloying are evident from SEM micrographs, which are shown in inset in **Figure 3**. From SEM micrographs, it can be seen clearly that the unmilled powders have different shapes and particle sizes. The Cu and Mg powder particles are of irregular shapes with an average size in the range of 50–150 μm. The Ni powder is a spherical morphology with size in the range of 20–60 μm. After 5 hours of milling, the powder particles of Cu–Mg–Ni alloy became nearly spherical shaped with an average size in the range of 10–30 μm. On further milling (10 hours milling), the homogeneity of the $Cu_{50}Mg_{25}Ni_{25}$ alloy increased and its particle size decreased up to 5 μm. For the higher milling time up to 25 hours, the formation of submicrometer particles was observed. Therefore, the average particle size was obviously determined below 5 μm.

http://dx.doi.org/10.5772/67404

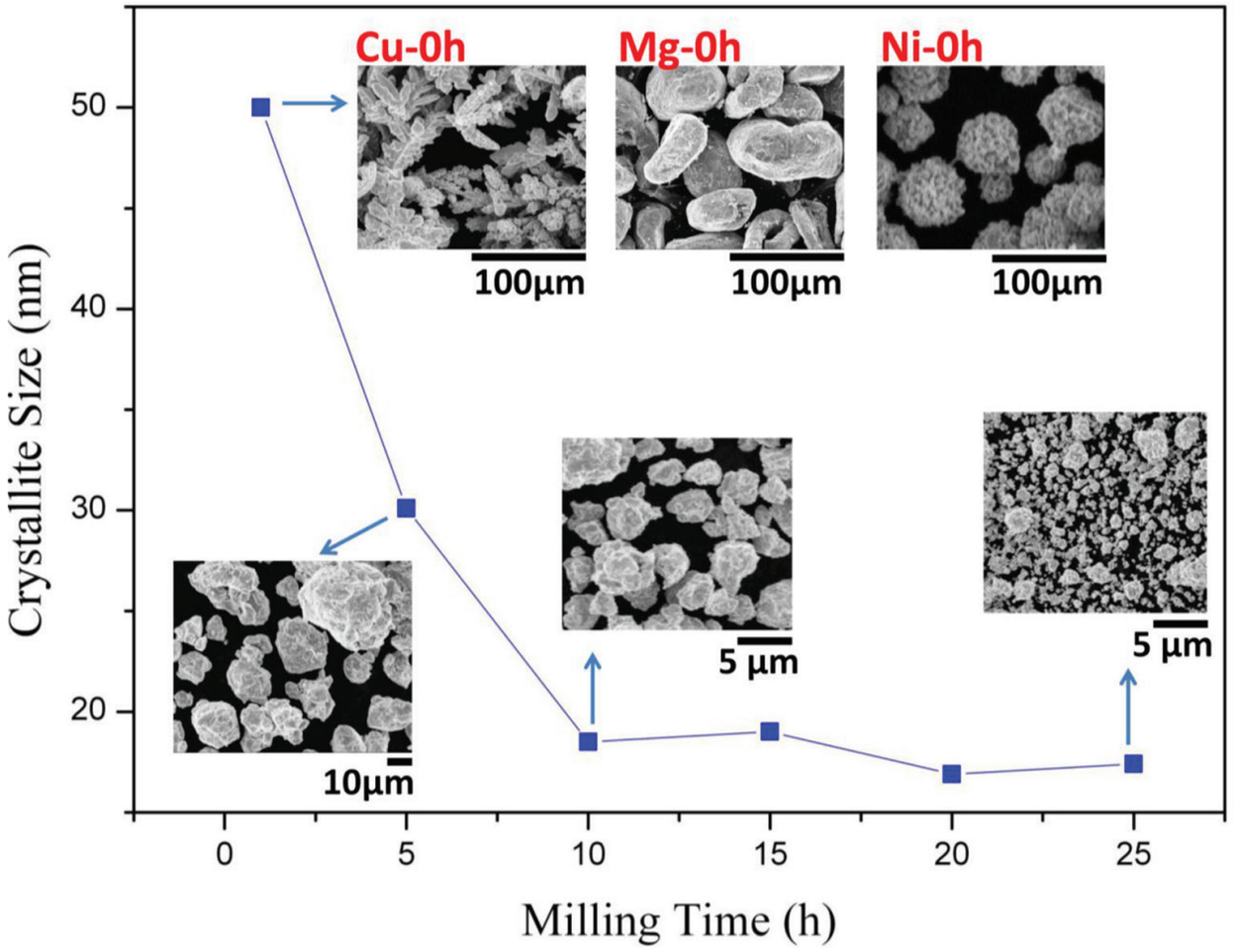

Figure 3. Crystal size of mechanically alloyed $Cu_{50}Mg_{25}Ni_{25}$ powders as a function of milling time and the insets: SEM micrographs of the powder particles after 0, 5, 10, and 25 hours of milling times.

The sample after 25 hours of milling was also investigated using transmission electron microscopy (TEM). Typical dark-field (DF) images are shown in **Figure 4(a** and **b)**. According to the TEM micrographs, the structure consists of nanocrystalline grains with the size of around 20 nm. **Figure 4(c)** illustrates the corresponding grain size distribution obtained using several DF images in order to have sufficient statistics (more than 240 grains). The obtained grain size distribution was fitted to the log-normal distribution function to calculate the mean average grain size. With the median m and the variance σ of the log-normal distribution function, the average grain sizes can be obtained according to the Eq. (2):

$$\langle x_j \rangle = m \exp(k\sigma^2) \tag{2}$$

With the k values of 0.5, 2.5, and 3.5 will give the arithmetic, area-weighted, and volume-weighted average grain size, respectively [16]. In order to compare with the results obtained by Rietveld refinement of XRD patterns and Debye-Scherrer equation, volume-weighed grain size was calculated to be 20 nm. This is in a good agreement with the values of 10 and 17.4 nm obtained by Rietveld refinement of XRD patterns and Debye-Scherrer equation, respectively. These results agree with a previous study which reported the production of similar compositions of Cu-Mg-Ni

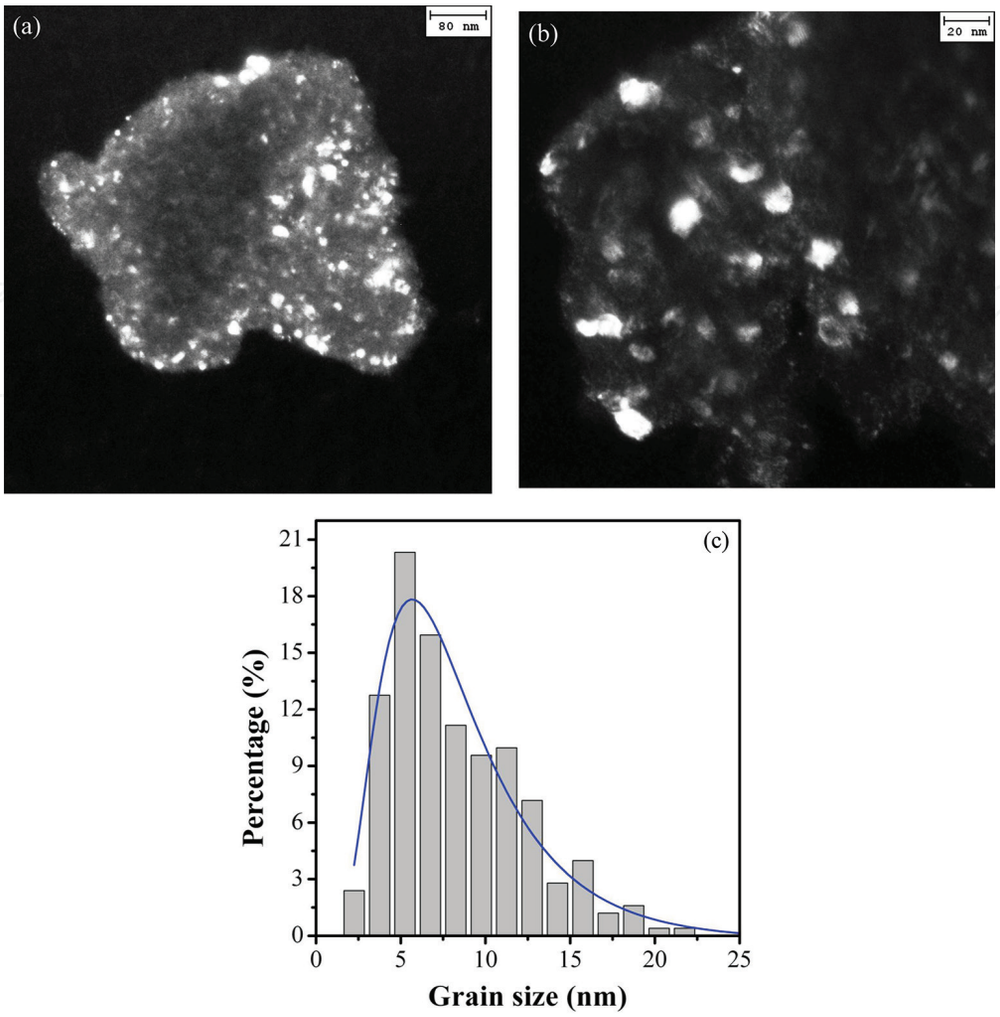

Figure 4. Dark field TEM micrographs of $Cu_{50}Mg_{25}Ni_{25}$ powders milled for (a), (b) 25 hours, and (c) the corresponding grain size distribution with the solid line as the fit to the log-normal distribution.

powders by the mechanical alloying, although the starting compositions were different being $Cu_{50}Mg_{30}Ni_{20}$ and $Cu_{50}Mg_{45}Ni_{5}$ [17].

Size calculations by TEM and XRD have been reported in many different systems, many often showing a large discrepancy between the size values obtained by TEM and XRD. Accordingly, the large discrepancy is due to the hierarchy of the deformed structure, details of which can be found elsewhere [16, 18]. This originates from the type of the information obtained by XRD and TEM, which are coherently scattering domain size (the smallest unfaulted peace of a crystal [19]) and grain size, respectively. Another reason giving rise to the discrepancy is the miscalculation of the coherent domain size by XRD that is due to the elastic anisotropy of the investigated materials [19]. The consequence of the presence of elastic anisotropy is that the strain broadening is not anymore a monotonous function of diffraction angle (2θ). New models have been developed in order to consider the effect of elastic anisotropy with the assumption that most of the strain originates from the presence of dislocations and the introduction of the concept of dislocation contrast factors [20, 21]. The effect of planar faults is also included in these models [20, 21]. The size values by XRD in this work are obtained without any special

http://dx.doi.org/10.5772/67404

considerations about elastic anisotropy or the presence of planar faults. However, there is a good agreement between the two values. A possible explanation is that the FCC solid solution formed during milling does not have a considerable substructure inside grains. According to diffraction patterns (**Figure 1(b)**), the reflections related to the FCC solid solution do not exist before 10 hours of ball milling. They emerge after 10 hours and their intensity increases by further milling. This suggests that they may form by some dynamic processes like dynamic recrystallization of defect-free small grains within the heavily strained matrix. The observation that the reflections do not exist before 10 hours of milling and amount of that increases by further milling, strengthens the idea of recrystallization. As a result, the structure is composed of nanosized grains with no substructure. It is also clear from the TEM micrographs of the final sample. The uniform diffraction of the electron beam by grains implies that they are substructure-free. The two size values obtained by XRD and TEM are in a good agreement because XRD gives the size of the substructure and that the grains do not contain any substructure.

Figure 5 shows lattice parameters of Cu-based FCC solid solution phase for $Cu_{50}Mg_{25}Ni_{25}$ alloy that had been mechanically alloyed for various milling times. As it is seen in **Figure 5**, the lattice parameters increase with increasing milling time. The increase of lattice parameter with milling time may be attributed to the effect of dissolving of bigger Mg atoms into Cu. It can be seen that the variation is sharp at the initial stage, however, after 15 hours milling it reaches a constant value. This indicates that the dissolution of Mg into Cu is fully completed. On the other hand, the effect of Ni to lattice parameter is very low because the atomic radii of Cu (0.128 nm) and Ni (0.125 nm) are close to each other. This provides a likely explanation of why the lattice parameter

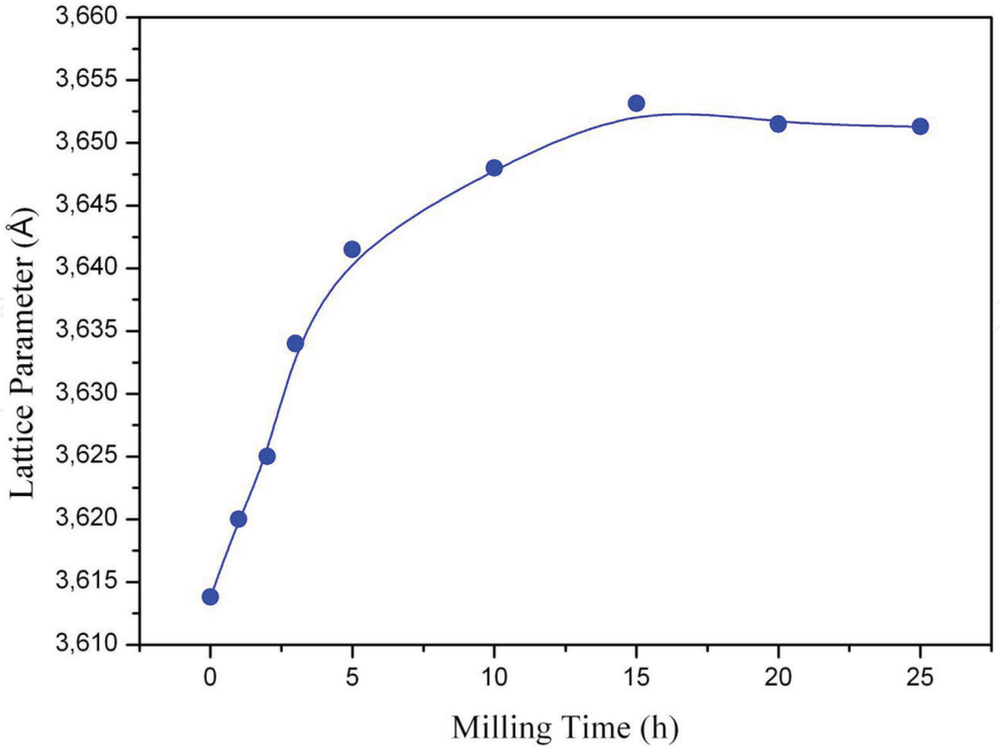

Figure 5. Lattice parameters of Cu-based FCC solid solution phase as a function of milling time. The line through the data points is a visual guide.

of Cu-based FCC solid solution phase increases from 3.61 to 3.65 Å during different stages of milling from 0 to 25 hours. For comparison, the lattice constant of MgO phase is 4.211 Å.

4. Conclusions

In this study, the nature of the phases formed and their particle sizes have been reported when the starting ternary mixture of Cu:Mg:Ni in the ratio of 50:25:25 is ball-milled for 25 hours. After 25 hours milling time, nanostructured Cu-based solid solution containing Cu, Mg, and Ni with FCC structure along with smaller quantities of FCC $Mg_{0.85}Cu_{0.15}$ and FCC MgO phases is formed. The crystallite size of this alloy was calculated by Debye-Scherrer and Rietveld Refinement methods using XRD data. In order to confirm the crystallite size obtained by XRD, the microstructure of the final powder was also monitored by TEM. The size value obtained by the TEM was determined to be 20 nm, which is in a good agreement with values determined from the analysis of the XRD pattern. This agreement is attributed to the formation of defect-free grains with no substructure during ball milling. It may be a possible mechanism of dynamic recrystallization for the emergence of such small grains (<20 nm). The morphology and particle size distribution of the $Cu_{50}Mg_{25}Ni_{25}$ alloy have been changed during mechanical alloying. The elemental powders, which have different shapes in the initial stage, became nearly rounded and the homogeneity increased with increasing milling time. The average particle size of the final product was determined to be below 5 μm. The remaining unresolved issues are the exact atomic concentrations of Cu, Mg, and Ni in the ternary alloy formed in this process here and in earlier studies reported in Ref. [17] and the nature of the phase diagram of the Cu, Mg, Ni system. These issues will be investigated in future studies.

Acknowledgements

The authors thank Kahramanmaras Sutcu Imam University for financial support of the research program (Project No:2011/3-21). One of the authors (C. Kursun) would like to thank the Council of Higher Education (YÖK) for graduate research support.

Author details

Celal Kursun[1]*, Musa Gogebakan[1], M. Samadi Khoshkhoo[2] and Jürgen Eckert[3]

*Address all correspondence to: celalkursun@ksu.edu.tr

1 Department of Physics, Faculty of Art and Sciences, Kahramanmaras Sutcu Imam University, Kahramanmaras, Turkey

2 IFW Dresden, Institute for Complex Materials, Dresden, Germany

3 Department of Materials Physics, Erich Schmid Institute of Materials Science, Austrian Academy of Sciences (ÖAW), Leoben, Austria

References

[1] M. Azimi, G.H. Akbari, Characterization of nano-structured Cu–6 wt.% Zr alloy produced by mechanical alloying and annealing methods, J Alloy Compd 555 (2013) 112-116.

[2] D. Zhao, Q.M. Dong, P. Liu, B.X. Kang, J.L. Huang, Z.H. Jin, Aging behavior of Cu–Ni–Si alloy, Mat Sci Eng A-Struct 361 (2003) 93-99.

[3] C. Suryanarayana, Mechanical alloying and milling, Prog Mater Sci 46 (2001) 1-184.

[4] C. Kursun, M. Gogebakan, Characterization of nanostructured Mg–Cu–Ni powders prepared by mechanical alloying, J Alloy Compd 619 (2015) 138-144.

[5] M.A. Meyers, A. Mishra, D.J. Benson, Mechanical properties of nanocrystalline materials, Prog Mater Sci 51 (2006) 427-556.

[6] T. Varol and A. Canakci, Effect of particle size and ratio of B_4C reinforcement on properties and morphology of nanocrystalline Al2024-B_4C composite powders, Powder Technol 246 (2013) 462-472.

[7] K. Shengzhong, F. Lui, D. Yutian, X. Guangji, D. Zongfu, L. Peiqing, Synthesis and magnetic properties of Cu-based amorphous alloys made by mechanical alloying, Intermetallics 12 (2004) 1115-1118.

[8] G. Wang, S. Fang, X. Xiao, Q. Hua, J. Gu, Y. Dong, Microstructure and properties of $Zr_{65}Al_{10}Ni_{10}Cu_{15}$ amorphous plates rolled in the super-cooled liquid region, Mater Sci and Engg A 373 (2004) 217-220.

[9] M. Gogebakan, The effect of Si addition on crystallization behaviour of amorphous Al-Y-Ni alloy, J Mater Eng Perform 13 (2004) 504-508.

[10] S. Deledda, J. Eckert, L. Schultz, Mechanical alloyed Zr-Cu-Al-Ni-C glassy powders, Mat Sci Eng A-Struct 375-377 (2004) 804-808.

[11] J. Guerrero-Paz, D. Jaramillo-Vigueras, Comparison of grain size distributions obtained by XRD and TEM in milled FCC powders, Nanostrcut Mater 11 (1999) 1195-1204.

[12] Y. Zhong, D.H. Ping, X.Y. Song, F.X. Yin, Determination of grain size by XRD profile analysis and TEM counting in nano-structured Cu, J Alloy Compd 476 (2009) 113-117.

[13] F. Hadef, A. Otomani, A. Djekoun, J.M. Grenèche, Structural and microstructural study of nanostructured $Fe_{50}Al_{40}Ni_{10}$ powders produced by mechanical alloying, Mater Charact 62 (2011) 751-759.

[14] M. Gogebakan, B. Avar, Quasicrystalline phase formation during heat treatment in mechanically alloyed $Al_{65}Cu_{20}Fe_{15}$ alloy, Mater Sci Tech Ser 26 (2010) 920-924.

[15] C. Suryanarayana, M. Grant Norton, X-ray Diffraction A Practical Approach, Plenum Press, New York (1998), p. 207.

[16] T. Ungár, G. Tichy, J. Gubicza, R.J. Hellmig, Correlation between subgrains and coherently scattering domains, Powder Diffr 20 (2005) 366-375.

[17] M. Gogebakan, C. Kursun, J. Eckert, Formation of new Cu-based nanocrystalline powders by mechanical alloying technique, Powder Technol 247 (2013) 172-177.

[18] M. Samadi Khoshkhoo, S. Scudino, J. Thomas, K.B. Surreddi, J. Eckert, Grain and crystallite size evolution of cryomilled pure copper, J Alloy Compd 509 (2011) 343–S347.

[19] E. Schafler, M. Zehetbauer, Characterization of nanostructured materials by X-ray line profile analysis, Rev Adv Mater Sci 10 (2005) 28-33.

[20] T. Ungár, A. Borbély, The effect of dislocation contrast on X-ray line broadening: A new approach to line profile analysis, Appl Phys Lett 69 (1996) 3173-3175.

[21] T. Ungár, Á. Révész, A. Borbély, Dislocations and grain size in electrodeposited nanocrystalline Ni determined by the modified Williamson-Hall and Warren-Averbach procedures, J. Appl. Cryst 31 (1998) 554-558.